Off-axis behavior of an infrared meander-line waveplate

Jeffrey S. Tharp,[1,3] Javier Alda,[2,*] and Glenn D. Boreman[1,4]

[1]*CREOL/College of Optics and Photonics, University of Central Florida, Orlando, Florida 32816, USA*
[2]*School of Optics, University Complutense of Madrid, Avenida Arcos de Jalón s/n, 28037 Madrid, Spain*
[3]*jstharp@creol.ucf.edu*
[4]*boreman@creol.ucf.edu*
[*]*Corresponding author: j.alda@opt.ucm.es*

Received July 6, 2007; revised August 20, 2007; accepted September 2, 2007;
posted September 5, 2007 (Doc. ID 84901); published September 27, 2007

An infrared meander-line waveplate has been modeled and measured over the 8 to 12 μm spectral band in terms of its differential phase delay, axial ratio of the output polarization ellipse, and power throughput for angles of incidence between 0° and 60°. The study has been performed for planes of incidence parallel and perpendicular to the meander-line axis. The main significance is that the phase delay remains almost unaffected by the angle of incidence. Infrared meander-line retarders can thus be used well beyond the paraxial range as in low-*f*/# optical systems and in non-normal-incidence applications. © 2007 Optical Society of America

OCIS codes: 260.1440, 260.5430.

Meander-line waveplates act as an anisotropic impedance layer and have been previously demonstrated as polarization-controlling elements in the infrared [1]. Incident radiation is decomposed into two orthogonal states. The component parallel to the meander-line axis experiences a primarily inductive impedance that advances the phase, while the orthogonal component experiences a primarily capacitive impedance that delays the phase [2]. Upon reradiation from the meander-line structure, the two orthogonal components are superimposed into a single wave with a different polarization state than the incident beam because of the differential phase delay. An interesting aspect of these structures is that the phase delay can be quite broadband, and this property led to further radio-frequency (RF)-band investigations into the performance of the structure under varying angles of incidence [3–5].

In optics, the operational conditions typically include a large angular spectrum of illumination, as in a low-*f*/# optical train, or the need to function under a nonzero angle of incidence, as in polarization beam splitters. Due to the geometry of the meander lines, the off-axis angular behavior is expected to depend on the orientation of the plane of incidence with respect to the meander lines. The goal of this contribution is to show how this dependence can be modeled and how an actual device working in the infrared behaves in off-axis conditions.

The single-layer meander-line structure investigated in this study was designed as a 90° phase retarder for the 8 to 12 μm infrared band [6]. The periodic nature of the array is represented by using a unit cell of finite geometry. The geometrical variables, as shown in Fig. 1(a), were pulse width (pw), pulse height (ph), width (w), and periodicity (dx). The design parameters were $w=0.6$ μm, $pw=0.9$ μm, $ph=0.8$ μm, and $dx=1.45$ μm. The constraints on the design of the meander-line structure included the expected resolution of the electron beam pattern generator and the optical properties of the substrate. High-resistivity silicon was used as a substrate to prevent electrical shorting of the meander-line arrays and because of inherent low attenuation in the band of interest. The metal used to write the meander lines was gold at a thickness of 130 nm.

Both for the measurements and modeling, the orientation of the plane of incidence was defined relative to the meander lines. The angle of the plane of incidence with respect to the meander lines, α, is defined as 0° for the plane of incidence lying parallel to the meander-line axis and 90° for the plane perpendicular to the meander-line axis. This geometry is depicted schematically in Fig. 1(b). Due to the lack of two-dimensional symmetry, it is expected that the behavior will be different for a given incident angle in each of these two orientations. A simple explanation for this differential behavior can be seen as following the change of the projected dimensions of the meander lines when varying the angle of incidence in the two planes of incidence. When the plane of incidence is parallel to the meander lines ($\alpha=0°$), the capaci-

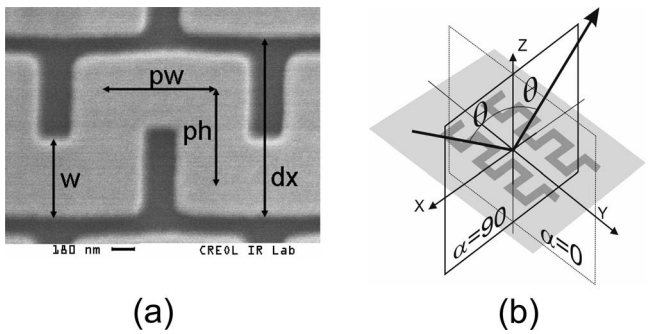

Fig. 1. (a) Scanning electron microscope micrograph of the meander-line structure analyzed in this paper, with geometric parameters labeled. (b) Coordinate orientation for the calculation and measurement of the off-axis incidence behavior of a meander line. For clarity, only light incident at an angle θ in the plane of incidence $\alpha=90°$ is shown.

0146-9592/07/192852-3/$15.00

tive contribution between adjacent meander lines remains constant, regardless of the value of the angle of incidence. However, for incidence in the plane $\alpha = 90°$, both the capacitive and inductance contributions vary with the angle.

The meander-line elements were modeled using the Ohio State Periodic Method of Moments computer code. The angular performance was expected to be stable, based upon previous work in the RF domain [7].

The meander-line element was measured in transmission over the 8 to 12 μm band using an infrared variable-angle spectroscopic ellipsometer for a range in the incidence angles between 0° and 60°. Measurements were made in 2° increments. The ellipsometric data were processed to obtain the phase delay between components, along with the axial ratio (AR) of the polarization ellipse when the structure was illuminated with linearly polarized light oriented at 45° with respect to the meander-line axis [8]. Both planes of incidence were also measured.

The phase delay shows that a change in the angle of incidence, θ, produces little effect over the band of interest (see Fig. 2 for $\theta = 0°$, 40°, and 60°). The effect is even less noticeable for the $\alpha = 90°$ orientation, where the predictions from the model show a more stable dependence. This performance allows for extending the use of these retarders well beyond the paraxial range without a significant departure in the phase delay introduced.

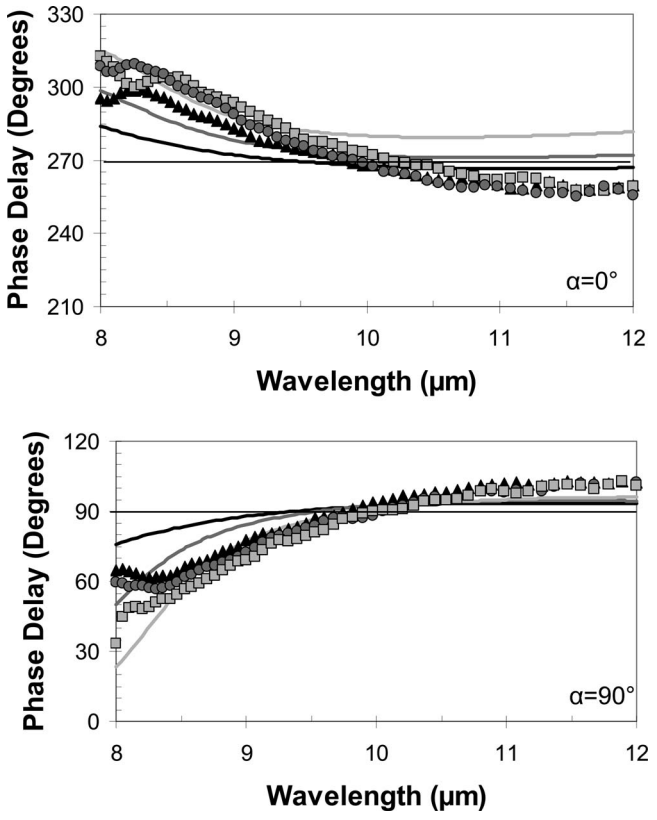

Fig. 2. Phase delay plots for the two orientations analyzed in this paper: $\alpha = 0°$ (top) and $\alpha = 90°$ (bottom). The prediction of the model is plotted as solid curves for three angles of incidence: $\theta = 0°$ (black curve), $\theta = 40°$ (dark gray), and $\theta = 60°$ (light gray). The experimental data are plotted as black triangles ($\theta = 0°$), dark gray circles ($\theta = 40°$), and light-gray squares ($\theta = 60°$).

The spectral dependence of the AR for three different incidence conditions ($\theta = 0°$, 40°, and 60°) is plotted in Fig. 3. It is observed that the difference in performance for the two orientations ($\alpha = 0°$ and $\alpha = 90°$) is related to the spectral location of the lower AR for each case (AR = 1 corresponds to circular polarization). In the case of $\alpha = 0°$, the smallest AR shifts toward shorter wavelengths as the angle of incidence increases. However, when illuminating in the plane $\alpha = 90°$, the lowest AR moves towards longer wavelengths with increasing angle of incidence. It is also observed that the average AR remains less than 3 over the whole spectral band in both planes of incidence for angles of incidence up to 40°.

We have also calculated the band-integrated spectral transmittance, defined as

$$T_{p,s}(\theta,\alpha) = \frac{\int_{8\ \mu\mathrm{m}}^{12\ \mu\mathrm{m}} T_{p,s}(\lambda,\theta,\alpha)\Phi_{\lambda,bb}(\lambda,T=300)\mathrm{d}\lambda}{\int_{8\ \mu\mathrm{m}}^{12\ \mu\mathrm{m}} \Phi_{\lambda,bb}(\lambda,T=300)\mathrm{d}\lambda}, \tag{1}$$

where $\Phi_{bb}(\lambda, T = 300)$ is the spectral power from a blackbody at 300 K. Then, $T_{p,s}(\theta,\alpha)$ expresses the in-band transmittance for thermal sources at room tem-

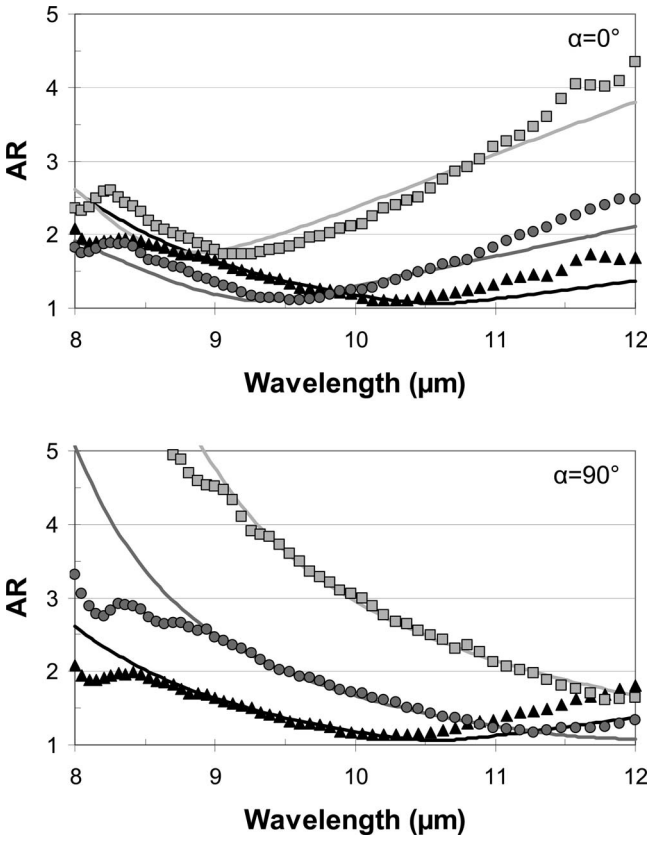

Fig. 3. Axial ratio plots for the case of a linearly polarized light oriented at 45° with respect to the meander-line orientation. The symbols and line conventions are the same as in Fig. 2.

perature as a function of the angle of incidence, θ, the orientation of the plane of incidence, α, and the orientation of the electric field, parallel (p) or perpendicular (s) to the plane of incidence. The results are given in Fig. 4, including linear polarizations and average polarizations in both planes of incidence. The average-polarization results can be applied in cases of unpolarized light, linearly polarized light oriented at 45°, and circularly polarized light. It is observed that the in-band transmittance is better bounded for the case of $\alpha=0°$ than for the case of $\alpha=90°$. The performance is shown to be quite stable, even for large angles of incidence. The average precision of our measured transmission coefficients in this band is ±0.003 as determined from analysis of the error bars on the measurement.

Though the angular performance of the integrated transmission is stable, it is observed that even at normal incidence the overall transmission of the meander-line retarder is about 14%. This low transmission is due to the impedance mismatches of the silicon and the meander-line structure with air. For a single-layer meander-line operating in free space as a 90° retarder, the resulting impedance mismatch will only ideally have a 50% transmission. When the dielectric permittivity (~11.5) of silicon is taken into account, the ideal transmission will become even lower, closer to 25% under ideal conditions of lossless metal. However, there are means to increase the transmission by using lower permittivity substrates and/or multiple layers of meander lines to reduce the impedance mismatch at each layer [6]. Both of these methods show promise of increasing the transmission to upwards of 70%, keeping the concept feasible in most applications.

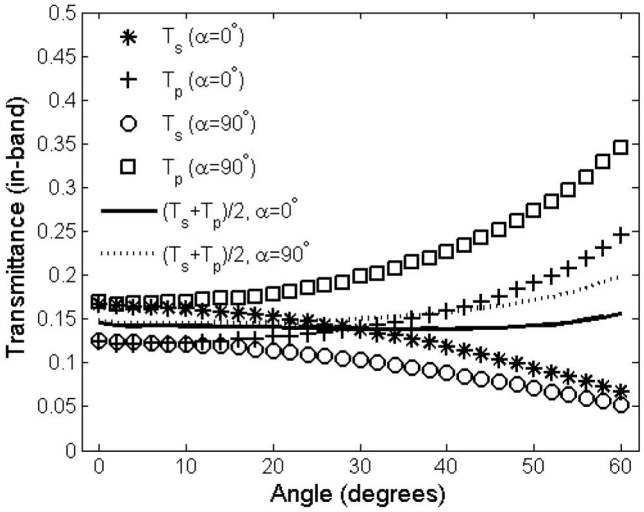

Fig. 4. Integrated (8 to 12 μm) transmittance as a function of angle of incidence for illumination by a 300 K blackbody.

In conclusion, the phase delay of meander-line retarders remains stable with respect to the angle of incidence, as was shown in both modeled and measured data. When illuminated with linearly polarized light at 45°, the minimum obtainable AR remains under 2, but for increasing angles of incidence the spectral location of this roundest ellipse of polarization moves towards shorter wavelengths for $\alpha=0°$ and towards longer wavelengths for $\alpha=90°$. The total integrated transmittance was calculated from measured power transmission coefficients, and the results show that, although the transmittance of the components of the field vary with the angle of incidence, the average remains constant within the paraxial range. Outside the paraxial range, the largest discrepancy appears for the incidence along the $\alpha=90°$ plane, reaching 33% more transmittance at $\theta=60°$ than in normal incidence. Finally, it may be concluded that the results presented in this paper clear the way for the use of meander-line retarders in low-f/# optical systems and for non-normal-incidence applications. Also, though this structure was designed to operate in transmission, a single-layer structure could be designed for good operation in reflection, particularly on a high-permittivity substrate.

J. Alda is grateful to the Ministerio of Educacion y Ciencia of Spain for financing his stay at the College of Optics and Photonics of the University of Central Florida through the programs PR2006-006 and TEC2006-1882.

References

1. J. S. Tharp, J. M. López-Alonso, J. C. Ginn, C. F. Middleton, B. A. Lail, B. A. Munk, and G. D. Boreman, Opt. Lett. **31**, 2687 (2006).
2. L. Young, L. Robinson, and C. Hacking, IEEE Trans. Antennas Propag. **21**, 376 (1973).
3. M. Mazur and W. Zieniutycz, in *13th International Conference on Microwaves, Radar, and Wireless Communications* (IEEE, 2000), pp. 78–81.
4. J. Zürcher, Microwave Opt. Technol. Lett. **18**, 320 (1998).
5. T. K. Wu, IEEE Microw. Guid. Wave Lett. **4**, 199 (1994).
6. J. S. Tharp, B. A. Lail, B. A. Munk, and G. D. Boreman, "Design and demonstration of an infrared meanderline phase retarder," IEEE Trans. Antennas Propag. (to be published).
7. B. A. Munk, *Finite Antenna Arrays and FSS* (Wiley-IEEE, 2003), appendix C.
8. D. Goldstein, *Polarized Light*, 2nd ed. (Marcel-Dekker, 2003).